Journal of Molecular Catalysis A: Chemical 319 (2010) 58–65

Contents lists available at ScienceDirect

Journal of Molecular Catalysis A: Chemical

journal homepage: www.elsevier.com/locate/molcata

# The catalytic function of $SiO_2$-immobilized Mn(II)-complexes for alkene epoxidation with $H_2O_2$

Ag. Stamatis [a], D. Giasafaki [a], K.C. Christoforidis [b], Y. Deligiannakis [b], M. Louloudi [a,*]

[a] Department of Chemistry, University of Ioannina, 45110 Ioannina, Greece
[b] University of Ioannina, Department of Environmental and Natural Resources Management, Laboratory of Physical Chemistry, Pyllinis 9, 30100 Agrinio, Greece

ARTICLE INFO

*Article history:*
Received 22 September 2009
Received in revised form
27 November 2009
Accepted 27 November 2009
Available online 21 December 2009

*Keywords:*
Catalytic epoxidation
Supported complexes
Manganese complexes
$H_2O_2$ activation
Modified silica

ABSTRACT

Two symmetrical acetylacetone-based Schiff bases were immobilized on a silica surface by grafting and sol–gel procedure. The corresponding supported manganese complexes were prepared and evaluated as heterogeneous catalysts for alkene epoxidation with $H_2O_2$. These heterogeneous catalysts show remarkable effectiveness and selectivity towards epoxide formation in the presence of ammonium acetate. Moreover, the developed heterogeneous catalysts preserve the coordination and catalytic properties of the active-homogeneous manganese catalysts for alkene epoxidation *vs.* the competitive $H_2O_2$ dismutation. EPR spectroscopy shows that in heterogeneous manganese catalysts the $Mn^{2+}$ centers are in a flexible, non-tight, coordination environment, as in the corresponding homogeneous manganese catalysts. However, after a first use of the heterogeneous catalysts, the Mn centers are detached from the ligand and are randomly dispersed on the $SiO_2$ surface. This is responsible for the loss of catalytic activity.



## 1. Introduction

Epoxidation reactions that involve hydrogen peroxide, which is still the 'greenest' terminal oxidant, is of great interest due to the importance of epoxides in the manufacture of both bulk and fine chemicals [1]. Despite success of homogeneous catalysts in the epoxidations, there is a clear demand for heterogeneous catalysts that provide advantages such as easy handling and product separation, catalyst recovery and less level of waste [2,3]. For these reasons, the development of heterogeneous catalysts for epoxidation reactions remains a very active field of research [4,5]. Preparation of heterogeneous catalysts, by covalent immobilization of transition-metal complexes on silica surface represents one of the most usable approaches [6–9]. Many of heterogeneous catalysts contain metal ions and chemically modified silica gels with active organic components [10]. Among the various transition-metals for heterogeneous catalytic epoxidation, manganese stands out as the most efficient, economical and environmental benign. Various manganese complexes immobilized on an inorganic matrix are known to be efficient and applicable as catalysts for the epoxidation of a wide range of alkenes [11–15]. However, the development of efficient manganese-systems that incorporate $H_2O_2$ has limitations due to competitive $H_2O_2$ dismutation by both the Mn center (catalase-type-activity) and the inorganic support. These limitations can explain why only a few such systems, based on supported manganese catalysts and $H_2O_2$, have been reported for alkene epoxidation [16–20].

Thus, efficient, cost effective and robust manganese catalysts remain at high demand in the field of hydrocarbon oxidation by $H_2O_2$. Within this context, during the last years, our group has developed imidazole based acetamide/Mn(II) systems [18,20] and acetylacetone-based Schiff bases/Mn(II) systems [19,21] as homogeneous and heterogeneous catalysts for alkene epoxidation with $H_2O_2$. More recently, we have presented homogeneous Mn(II)-catalysts with new symmetrical acetylacetone-based Schiff bases [22]. Their catalytic efficiency was shown to be switched-on by ammonium acetate achieving remarkable effectiveness and selectivity towards epoxides [22]. EPR spectroscopy provided evidence that the catalytic centers are mononuclear Mn(II) complexes with a flexible ligand-field environment [22].

Herein, the symmetrical acetylacetone-based Schiff bases are immobilized on a silica surface by grafting and sol–gel procedure. The obtained supported manganese complexes have been evaluated as catalysts for alkene epoxidation with $H_2O_2$ and compared with the corresponding homogeneous systems. EPR spectroscopy has been also used to study the coordination environment of the heterogeneous Mn-catalysts.

## 2. Experimental

All substrates were purchased from Aldrich, in their highest commercial purity, stored at 5 °C and purified by passage through

* Corresponding author. Tel.: +30 26510 08418; fax: +30 26510 08786.
*E-mail address:* mlouloud@uoi.gr (M. Louloudi).

1381-1169/$ – see front matter © 2009 Elsevier B.V. All rights reserved.
doi:10.1016/j.molcata.2009.11.021

a column of basic alumina with methanol as the eluting solvent, prior to use. Hydrogen peroxide was 30% aqueous solution.

Elemental analyses (C, H, N) were obtained using a Perkin-Elmer Series II 2400 elemental analyser. The manganese amount was determined by flame atomic absorption spectroscopy on a Perkin-Elmer AAS-700 spectrometer. Infrared spectra were recorded on a Spectrum GX Perkin-Elmer FT-IR System. Continuous-wave (c.w.) Electron Paramagnetic Resonance (EPR) spectra were recorded with a Brucker ER200D spectrometer at liquid $N_2$ temperature, equipped with an Agilent 5310A frequency counter. The spectrometer was running under a home-made software based on LabView. Diffuse reflectance UV–Vis spectra were recorded at room temperature on a Shimadzu UV-2401PC with a $BaSO_4$ coated integration sphere. Thermogravimetric analyses were carried out under atmosphere using Shimadzu DTG-60 analyser. GC analysis was performed using an 8000 Fisons chromatograph with a flame ionization detector and a Shimadzu GC-17A gas chromatograph coupled with a GCMS-QP5000 mass spectrometer. The $N_2$ adsorption–desorption isotherms were measured at 77 K on a Sorptomatic 1990, thermo Finnigan porosimeter. Specific surface areas were determined with the Brunauer–Emmett–Teller (BET) method using adsorption data points in the relative pressure ($P/P_0$) range of 0.05–0.30 and assuming a closely packed BET monolayer. $H_2O_2$ was added by a digitally controlled syringe pump type SP101IZ WPI over 1 h under stirring. Solution potential $E_h$ was measured by a Metrohm platinum redox electrode (type 6.0401.100).

### 2.1. Ligand synthesis

Ligands **1** and **2** have been synthesized and characterized recently [22].

### 2.2. Grafting procedure

In a typical synthesis, 2.0 mmol of **1** or **2** and 1.7 mmol of (3-chloropropyl)-trimethoxysilane were stirred for 48 h in 50 ml of MeOH under $N_2$ at 60 °C. To this solution 3.0 g of $SiO_2$ and 5 ml of EtOH were added, and the slurred solution maintained at 60 °C under $N_2$ for 24 h. Filtering gave **G-1** or **G-2**, respectively. The resulting materials were washed with MeOH and EtOH; they were further purified with EtOH using the soxhlet extraction method and dried under reduced pressure at 80 °C for 12 h. The loading achieved is *ca.* 0.28 mmol $g^{-1}$ for **G-1** and 0.26 mmol $g^{-1}$ for **G-2** determined, in both cases, by thermogravimetric and elemental analysis.

**G-1**: DRIFTS-IR ($cm^{-1}$, selected peaks): 1652: $\nu$(C=O); 1618: $\nu$(C=N); 1516: $\nu$(C=C); 1463: $\delta$(C–H); 1410: $\nu$(C–O). DRS ($\lambda_{max}$ (nm)): 232, 313, 491.

**G-2**: DRIFTS-IR ($cm^{-1}$, selected peaks): 1656: $\nu$(C=O); 1619: $\nu$(C=N); 1511: $\nu$(C=C); 1465: $\delta$(C–H); 1410: $\nu$(C–O); 1212: $\nu(CF_3)$. DRS ($\lambda_{max}$ (nm)): 228, 320, 489.

### 2.3. Metalation procedure

Approximately 0.3 mmol of $MnCl_2{\cdot}4H_2O$ or $Mn(CH_3COO)_2{\cdot}4H_2O$ and 0.5 g of **G-1** or **G-2** were stirred in MeOH overnight before filtering. To remove any weakly coordinated metal, the metalated materials, **G-1Mn$^{II}$Cl**, **G-1Mn$^{II}$acet**, **G-2Mn$^{II}$Cl** and **G-2Mn$^{II}$acet**, were exhaustively washed with MeOH, EtOH and $Et_2O$ and dried at 60 °C for 3 h. The amount of manganese was determined by back-titration of the remaining amount of metal ion into the solution and by atomic absorption spectroscopy.

**G-1Mn$^{II}$Cl**: Metal loading: 0.26 mmol $g^{-1}$. DRIFTS-IR ($cm^{-1}$, selected peaks): 1706: $\nu$(C=O); 1658: $\nu$(C=N); 1406: $\nu$(C–O). DRS ($\lambda_{max}$ (nm)): 230, 315, 483. This material had an average surface area of *ca.* 203 $m^2$ $g^{-1}$.

**G-1Mn$^{II}$acet**: Metal loading: 0.28 mmol $g^{-1}$. DRIFTS-IR ($cm^{-1}$, selected peaks): 1704: $\nu$(C=O); 1645: $\nu$(C=N); 1548: $\nu_{sym}(COO^-)$; 1441: $\nu_{as}(COO^-)$; 1408: $\nu$(C–O). DRS ($\lambda_{max}$ (nm)): 229, 310, 489. This material had an average surface area of *ca.* 286 $m^2$ $g^{-1}$.

**G-2Mn$^{II}$Cl**: Metal loading: 0.24 mmol $g^{-1}$.DRIFTS-IR ($cm^{-1}$, selected peaks): 1704: $\nu$(C=O); 1645: $\nu$(C=N); 1406: $\nu$(C–O); 1209: $\nu(CF_3)$. DRS ($\lambda_{max}$ (nm)): 227, 325, 476. This material had an average surface area of *ca.* 198 $m^2$ $g^{-1}$.

**G-2Mn$^{II}$acet**: Metal loading: 0.25 mmol $g^{-1}$.DRIFTS-IR ($cm^{-1}$, selected peaks): 1706: $\nu$(C=O); 1645: $\nu$(C=N); 1528: $\nu_{sym}(COO^-)$; 1441: $\nu_{as}(COO^-)$;1402: $\nu$(C–O); 1209: $\nu(CF_3)$. DRS ($\lambda_{max}$ (nm)): 227, 324, 487. This material had an average surface area of *ca.* 277 $m^2$ $g^{-1}$.

### 2.4. Sol–gel procedure

By adaptation of grafting-methodology used, 1.2 mmol of **1** and 1.0 mmol of (3-chloropropyl)-trimethoxysilane were stirred for 48 h in 10 ml of MeOH under $N_2$ at 60 °C in order to generate **OS-1** silicon precursor. After cooling, to this solution 2.4 mmol of $MnCl_2{\cdot}4H_2O$ were added. The obtained solution was stirred overnight at room temperature under $N_2$ leading to metalated precursor **OS-1Mn$^{II}$Cl**. The **S-1Mn$^{II}$Cl** catalyst was prepared by sol–gel method, through hydrolysis of TEOS and **OS-1Mn$^{II}$Cl** precursor in MeOH–$H_2O$ mixture in the presence of NaF as catalyst. For this, to the precursor solution 4.5 ml TEOS, 3.6 ml $H_2O$ and 4.2 mg NaF were added and mixed together for 10 min. The final molar ratio silicon precursor:NaF:TEOS:$H_2O$ was equal to 1:0.1:20:200. The gelation of the sol was observed in the next 3 h and the obtained gel was kept for aging for 3 days at room temperature. The filtered solid was extensively washed with water and methanol. The **S-1Mn$^{II}$Cl** material was further purified with MeOH using the soxhlet extraction method and dried under reduced pressure at 60 °C for 12 h. The loading achieved is *ca.* 0.19 mmol $g^{-1}$ determined by thermogravimetric and elemental analysis.

**S-1Mn$^{II}$Cl**: Metal loading: 0.20 mmol $g^{-1}$. DRIFTS-IR ($cm^{-1}$, selected peaks): 1686: $\nu$(C=O); 1658: $\nu$(C=N); 1403: $\nu$(C–O). DRS ($\lambda_{max}$ (nm)): 244, 315, 480. This material had an average surface area of *ca.* 465 $m^2$ $g^{-1}$.

### 2.5. Representative catalytic conditions

The alkene (1 mmol), acetophenone or bromobenzene (internal standard, 1 mmol), catalyst (1 μmol) and $CH_3COONH_4$ additive (1 mmol) in a acetone/MeOH (450 μl/400 μl) solvent mixture were cooled to 0 °C. $H_2O_2$ (2 mmol) was added by a digitally controlled syringe pump type SP101IZ WPI over 1 h under stirring. 10 min later, the test tube was removed from the ice bath and allowed to warm to room temperature 26 ± 1 °C. The progress of the reaction was monitored by GC–MS, for small samples taken from the reaction mixture. GC analysis of the solution provided the substrate conversion and product yield relative to the internal standard integration. To establish the identity of the epoxide product unequivocally, the retention time and spectral data were compared to those of an authentic sample. Blank experiments showed that without Mn-catalyst or $CH_3COONH_4$, epoxidation reactions do not take place.

## 3. Results and discussion

### 3.1. Synthesis of the materials

Immobilization of the ligands **1** and **2** requires their derivatization which occurs *via* phenolic groups with (3-chloropropyl)-trimethoxysilane (Scheme 1). The propyl-trimethoxysilane moiety

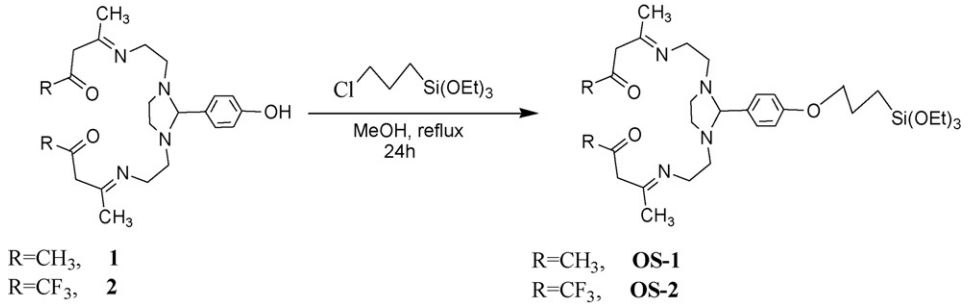


**Scheme 1.** Silane-derivatization of the ligands **1** and **2**.

of silicon precursors **OS-1** and **OS-2** allows covalent attachment of **1** and **2** on the silica surface.

Two methods of covalent attachment were applied: grafting on silica surface and sol–gel procedure providing materials **G** and **S**, respectively (Scheme 2). (i) The grafting involved attachment of **1** and **2** to the support surface to form hybrid materials **G-1** and **G-2** with covalently attached ligands. Soxhlet extractions of **G-1** and **G-2** ensure that only the covalently attached ligand molecules remain on the support. Metalation of these materials with 2 equiv. of $MnCl_2$ or $Mn(CH_3COO)_2$ per ligand molecule in methanol, gave **G-1Mn$^{II}$Cl**, **G-1Mn$^{II}$acet**, **G-2Mn$^{II}$Cl** and **G-2Mn$^{II}$acet**, after removal of any weakly associated metal with exhaustively washings. (ii) A modified sol–gel procedure involved an initial formation of metalated precursor **OS-1Mn$^{II}$Cl** followed by hydrolysis and co-condensation in the presence of TEOS to yield **S-1Mn$^{II}$Cl**. The catalytic epoxidation reactivity of all prepared materials **G-1Mn$^{II}$Cl**, **G-1Mn$^{II}$acet**,

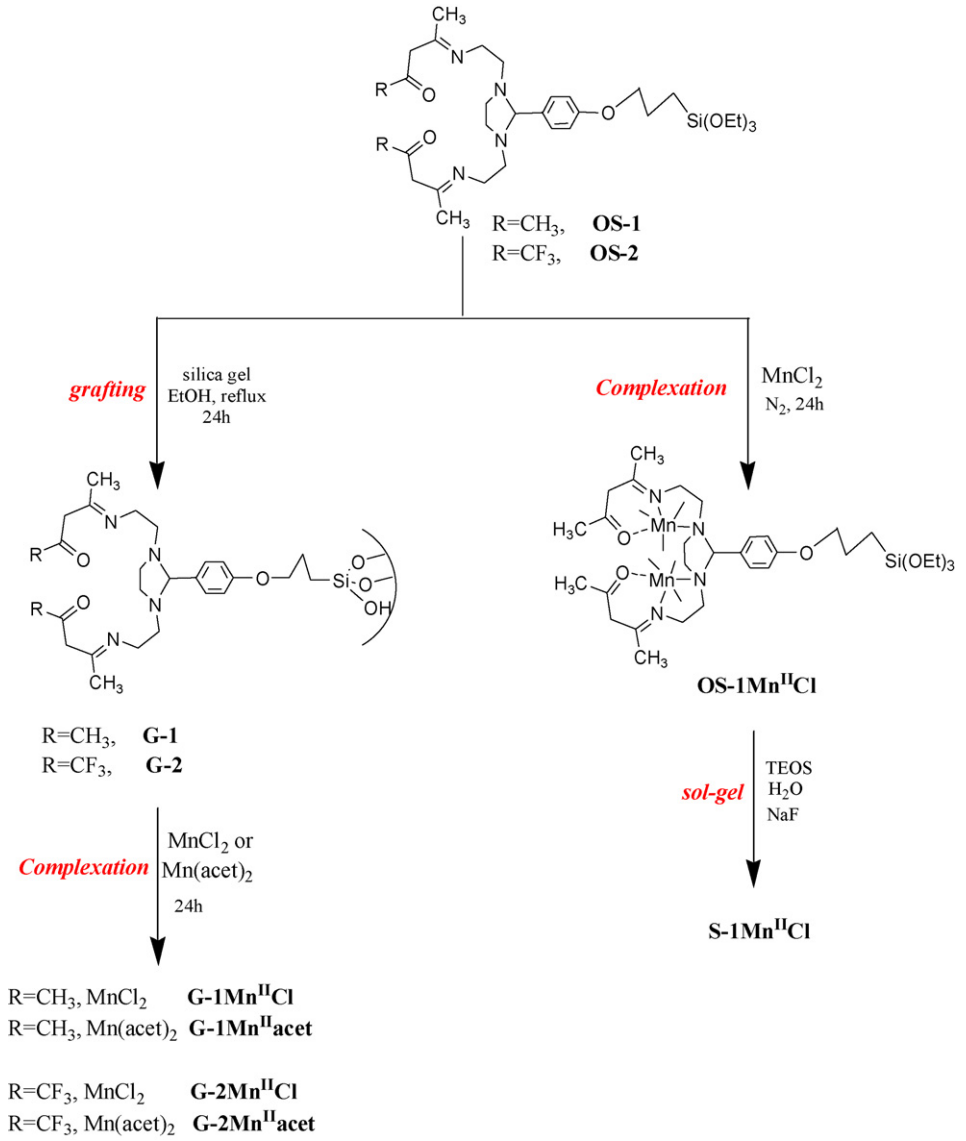


**Scheme 2.** Schematic representation of the synthesis of manganese catalysts.

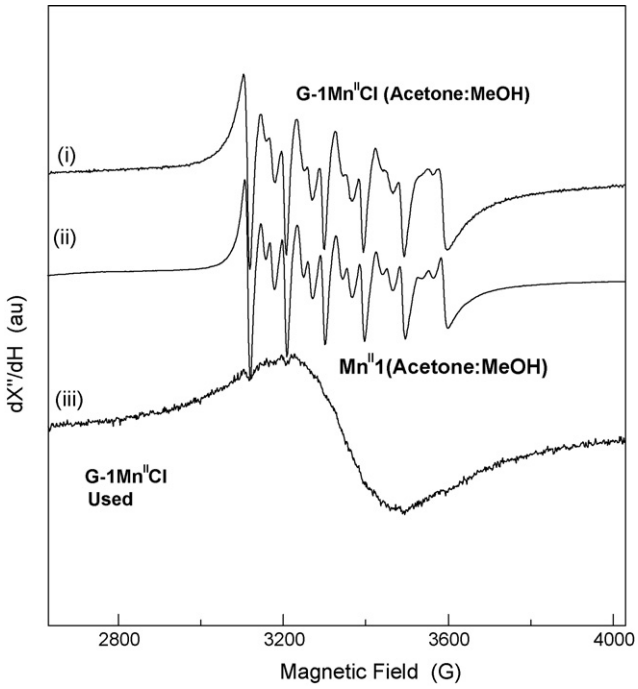


**Fig. 1.** EPR spectra of (i) homogeneous **Mn$^{II}$1** system in acetone/MeOH (1/1, v/v), (ii) unused heterogeneous **G-1Mn$^{II}$Cl** catalyst in MeOH and (iii) recycled heterogeneous **G-1Mn$^{II}$Cl** catalyst in MeOH. Experimental conditions: temperature 77 K, modulation amplitude 5 G, microwave power 10 dB.

**G-2Mn$^{II}$Cl**, **G-2Mn$^{II}$acet** and **S-1Mn$^{II}$Cl** are compared herein. When the sol–gel procedure applied, starting with a covalent immobilization of the ligand into the silica network, followed by metalation, the materials obtained were inactive in catalytic epoxidations.

The DRIFTS-IR-spectra of the synthesized materials show several bands corresponding to various structural units of the solids. In the IR-spectra of **G-1** and **G-2**, the bands at 1652 and 1656 cm$^{-1}$, respectively are attributed to the $\nu$(C=O) stretching vibrations; accordingly the bands observed in both spectra, at ~1618 cm$^{-1}$ to the $\nu$(C=N) stretching. Anchoring of the ligands **1** and **2** on the silica surface can be conveniently followed also by DR UV spectroscopy; in the corresponding spectra, the presence of the $\pi \rightarrow \pi^*$ transitions attributed to the immobilized ligands can be seen. In the IR-spectra of the metalated materials **G-1Mn$^{II}$Cl**, **G-1Mn$^{II}$acet**, **G-2Mn$^{II}$Cl**, **G-2Mn$^{II}$acet**, the C=O and C=N stretching vibrations are clearly shifted when compared with the corresponding non-metalated materials **G-1** and **G-2**, indicating coordination of manganese with the imine-nitrogen and the keto-oxygen of the immobilized ligands **1** and **2**. This is also supported by DR UV spectra. The **S-1Mn$^{II}$Cl** material presents the C=O and C=N stretching vibrations at about 1686 and 1658 cm$^{-1}$.

Fig. 1(i) shows a 77K EPR spectrum for the heterogeneous **G-1Mn$^{II}$Cl** in [acetone/MeOH]. For comparison, an EPR spectrum for the homogeneous **Mn$^{II}$1** in [aceteone/MeOH] is also displayed, Fig. 1(ii).

The EPR spectrum of **G-1Mn$^{II}$Cl** (Fig. 1, spectrum (i)) corresponds to mononuclear $Mn^{2+}$ ($S = 5/2$, $I = 5/2$) centers [23]. Analysis of the EPR spectrum based on the splittings of the semiforbidden EPR transitions, using the method of Misra [24] or the intensity method of Allen [25] as described previously [22] shows that that the Zero-Field Splitting (ZFS) parameter for **G-1Mn$^{II}$Cl** is $D = 0.40 \pm 0.5$ GHz. The $D$-value for the homogenous **Mn$^{II}$1** complex is $D = 0.38 \pm 0.5$ GHz [22]. This shows that the ligands around the $Mn^{2+}$ centers are slightly more strongly bound to the $Mn^{2+}$.

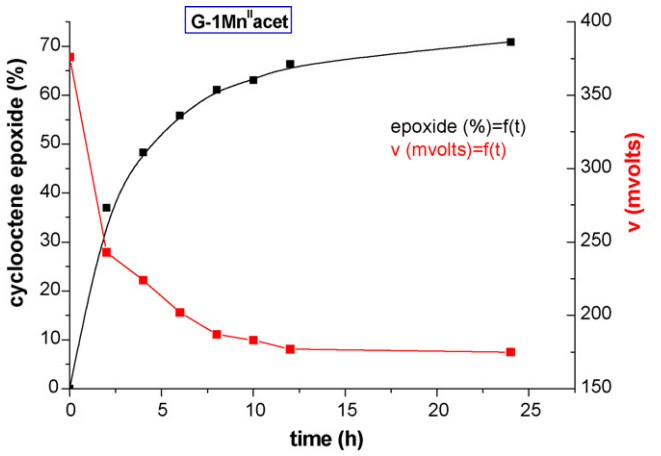


**Fig. 2.** Time dependence of cyclooctene epoxidation [black line] and solution redox potential [red line] for the same reaction catalysed by **G-1Mn$^{II}$acet**. (For interpretation of the references to color in this figure caption, the reader is referred to the web version of the article.)

### 3.2. Catalytic epoxidation with $H_2O_2$

To evaluate the catalytic behaviour of the prepared materials, oxidations of several alkenes have been carried out at room temperature. As in the case of homogeneous manganese catalysts [22], the present heterogeneous catalyst required also ammonium acetate as additive to produce efficient catalytic systems.

According to our data, the catalytic reactions were practically accomplished within 18 h. The time course profiles of the **G-1Mn$^{II}$acet**- and **G-2Mn$^{II}$acet**-catalysed epoxidations of cyclooctene, in conjunction with the observed redox potential of solution $E_h$ (*vs.* standard hydrogen electrode SHE) are given in Figs. 2 and 3. At the beginning of the reaction catalysed by **G-1Mn$^{II}$acet**, $E_h$ was +376 mV; after 2 h, it dropped at +243 mV with a 37% epoxide yield and finally, after a reaction time of 18 h, it approached a value of $E_h$ = +175 mV with a 71% yield. In the case of **G-2Mn$^{II}$acet**-catalysed epoxidation, at reaction time $t = 0$, $E_h$ was +383 mV, at $t = 2$ h, then decreased at +246 mV providing a product yield of 36% and at $t = 18$ h, $E_h$ approached +178 mV with a 70% cyclooctene epoxide formation. Additions of new amounts of oxidant slightly increased the $E_h$ resulting in an additional 5% epoxidation of the remaining substrate.

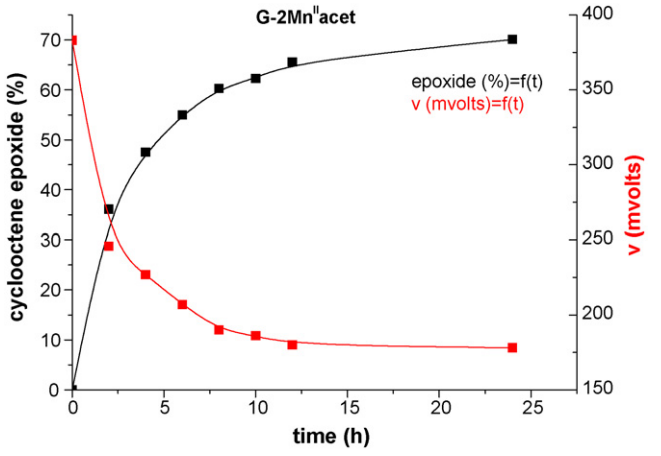


**Fig. 3.** Time dependence of cyclooctene epoxidation [black line] and solution redox potential [red line] for the same reaction catalysed by **G-2Mn$^{II}$acet**. (For interpretation of the references to color in this figure caption, the reader is referred to the web version of the article.)

**Table 1**
Alkene epoxidations catalysed by supported manganese complexes in the presence of $H_2O_2$[a].

| Substrate | Products | $MnCl_2$[b] | | | **G-1Mn$^{II}$Cl** | | | **S-1Mn$^{II}$Cl** | | | **G-2Mn$^{II}$Cl** | | | $Mn(acet)_2$[b] | | | **G-1Mn$^{II}$acet** | | | **G-2Mn$^{II}$acet** | | |
|---|---|---|---|---|---|---|---|---|---|---|---|---|---|---|---|---|---|---|---|---|---|---|
| | | Yield[e] | TON[d] | TOF (%) ($h^{-1}$)[c] | Yield[e] | TON[d] | TOF (%) ($h^{-1}$)[c] | Yield[e] | TON[d] | TOF (%) ($h^{-1}$)[c] | Yield[e] | TON[d] | TOF (%) ($h^{-1}$)[c] | Yield[e] | TON[d] | TOF (%) ($h^{-1}$)[c] | Yield[e] | TON[d] | TOF (%) ($h^{-1}$)[c] | Yield[e] | TON[d] | TOF (%) ($h^{-1}$)[c] |
| Cyclohexene | *cis*-Epoxide | 13.1 | | | 40.5 | | | 49.0 | | | 29.6 | | | 12.4 | | | 56.4 | | | 53.0 | | |
| | 2-Cyclohexenone | 0.4 | | | 2.5 | | | 4.1 | | | 2.8 | | | 0.4 | | | 3.0 | | | 4.0 | | |
| | 2-Cyclohexenol | 0.2 | 137 | 6 | 1.1 | 474 | 26.3 | 2.2 | 562 | 31.2 | 1.5 | 353 | 19.6 | 0.2 | 131 | 5 | 2.3 | 685 | 38.1 | 2.8 | 640 | 35.6 |
| | *cis*-Diol | – | 3.3 | 0.9 | 1.4 | 0.1 | 6.8 | 4.2 | | | | | | | | | | | | | | |
| Cyclooctene | *cis*-Epoxide | 18.0 | 180 | 8 | 58.6 | 586 | 32.6 | 51.0 | 510 | 28.3 | 49.7 | 497 | 27.6 | 16.8 | 168 | 7 | 70.9 | 709 | 39.4 | 70.1 | 701 | 38.9 |
| Hexene-1 | *cis*-Epoxide | 4.6 | 46 | 2 | 9.5 | 95 | 5.3 | 14.0 | 140 | 7.8 | 9.3 | 93 | 5.2 | 4.1 | 41 | 2 | 10.0 | 100 | 5.6 | 10.0 | 100 | 5.6 |
| Styrene | Epoxide | 17.1 | 171 | 7 | 47.6 | 476 | 26.4 | 16.0 | 178 | 9.9 | 15.3 | 159 | 8.8 | 12.4 | 124 | 5 | 46.7 | 475 | 26.4 | 19.2 | 222 | 12.3 |
| | Phenyl-acetaldehyde | – | | | – | | | 1.8 | | | 0.6 | | | – | | | 0.8 | | | 3.0 | | |
| *trans*-Methyl-styrene | *trans*-Epoxide | 14.3 | 143 | 6 | 22.5 | 241 | 13.4 | 21.5 | 240 | 13.3 | 21.6 | 239 | 13.3 | 14.9 | 149 | 6 | 52.9 | 542 | 30.1 | 54.3 | 590 | 32.8 |
| | *trans*-Methyl-ketone | – | | | 1.6 | | | 2.5 | | | 2.3 | | | – | | | 1.3 | | | 4.7 | | |
| Limonene[f] | 1,2-Epoxides | 21.0 | | | 50.8 | | | 33.5 | | | 49 | | | 20.4 | | | 74.0 | | | 71.2 | | |
| | | (11.8/9.2) | | | (27.9/22.9) | | | (18.5/15) | | | (26.8/22.2) | | | (11.7/8.7) | | | (41.5/32.5) | | | (38.9/32.3) | | |
| | (*cis*-/*trans*-) | 3.3 | | | 10.1 | | | 6.4 | | | 10.4 | | | 3.2 | | | 13.5 | | | 13.8 | | |
| | 8,9-Epoxides | 0.1 | 243 | 10 | 0.7 | 624 | 34.7 | 1.7 | 435 | 24.2 | 1.1 | 613 | 34.1 | 0.1 | 237 | 10 | 0.9 | 895 | 49.7 | 2.0 | 881 | 48.9 |
| | -Alcohol | | | | 0.8 | | | 1.0 | | | 0.8 | | | | | | 1.1 | | | 1.1 | | |
| | -Ketone di-epoxide | | – | | | | | 0.9 | | | | | | | | | | | | | | |
| *cis*-Stilbene | *cis*-Epoxide | 17.1 | | | 10.2 | | | 9.3 | | | 24.0 | | | 16.6 | | | 21.9 | | | 24.5 | | |
| | *trans*-Epoxide | 2.6 | 200 | 8 | 1.3 | 124 | 6.9 | 2.7 | 128 | 7.1 | 3.3 | 305 | 16.9 | 2.6 | 194 | 8 | 3.0 | 265 | 14.7 | 4.2 | 320 | 17.8 |
| | -ketone | 0.3 | 0.9 | 0.8 | 3.2 | 0.2 | 1.6 | 3.3 | | | | | | | | | | | | | | |

[a] Conditions: ratio of catalyst:$H_2O_2$:$CH_3COONH_4$:substrate = 1:2000:1000:1000; equivalent of catalyst = 1 μmol in 0.85 ml $CH_3COCH_3$:$CH_3OH$ (0.45:0.40). Reactions were completed within 18 h.
[b] $MnCl_2$ and $Mn(acet)_2$ have been evaluated as catalysts in homogeneous conditions. Reactions were completed within 24 h.
[c] TOF: turnover frequency which is calculated by the expression [epoxide]/[catalyst] × time ($h^{-1}$).
[d] TON: total turnover number, moles of products formed per mole of catalyst.
[e] Yields based on starting substrate and products formed. The mass balance is 98–100%.
[f] Limonene 1,2-oxide was found as a mixture of *cis*- and *trans*-isomers and limonene 8,9-oxide as a mixture of two diastereoisomers.

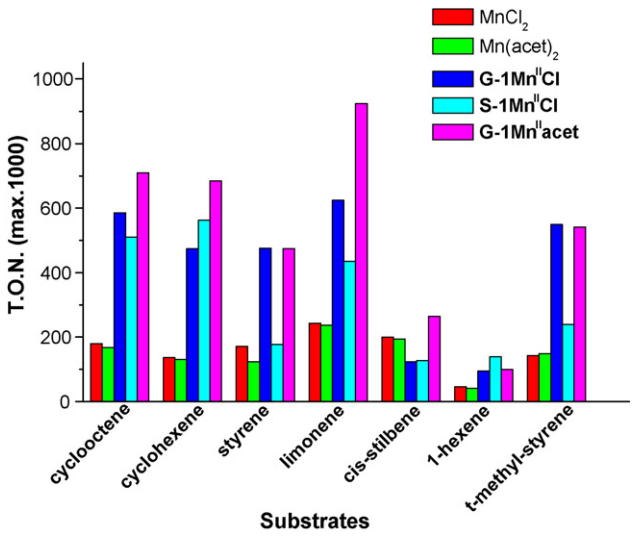


**Fig. 4.** Bar chart representation of alkene epoxidations catalysed by $MnCl_2$, $Mn(acet)_2$, **G-1Mn$^{II}$Cl**, **S-1Mn$^{II}$Cl** and **G-1Mn$^{II}$acet** in the presence of $H_2O_2$. Reaction performed in $CH_3COCH_3/CH_3OH$ (0.45:0.40 ml). See Table 1 for details.

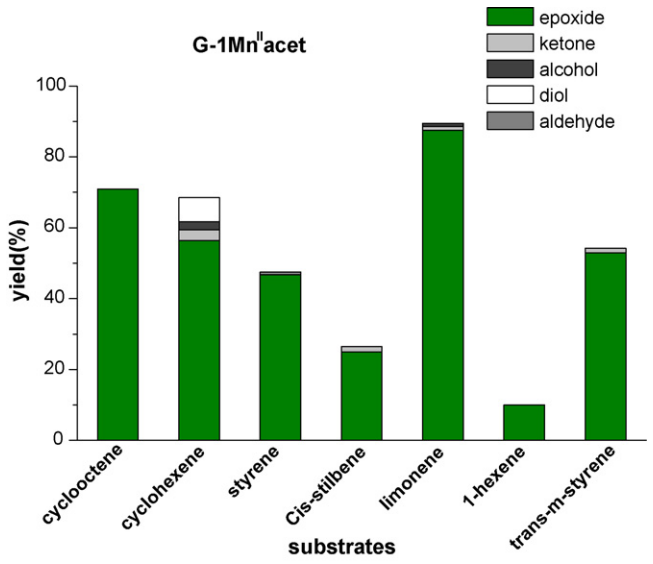


**Fig. 6.** Distribution of oxidation products catalysed by **G-1Mn$^{II}$acet** in the presence of $H_2O_2$. Reaction performed in $CH_3COCH_3/CH_3OH$ (0.45:0.40 ml). See Table 1 for further details.

According to the data in Table 1, epoxidation of a wide range of olefins proceeds with high conversion and selectivity for the epoxide product (the mass balance is 98–100%) was achieved in most of the cases (Table 1). For example, oxidation of cyclooctene provides a 100% selectivity for *cis*-cyclooctene epoxide with 58.6%, 49.7% and 51.0% yield and 100% m.b. catalysed by **G-1Mn$^{II}$Cl**, **G-2Mn$^{II}$Cl**, and **S-1Mn$^{II}$Cl**, respectively (see Figs. 4 and 5). When the **G-1Mn$^{II}$acet**, and **G-2Mn$^{II}$acet** catalysts were used, the *cis*-epoxide was also the only product and the obtained yields were 70.9% and 70.1% (see Figs. 4 and 5).

Hexene-1 is a rather hard oxidation substrate showing epoxide yields from 9.3% to 14.0% and selectivity 100% for the *cis*-epoxide. Cyclohexene achieves moderate epoxide yields, ranging from 29.6% to 56.4%. In addition, small amounts of the corresponding diol, probably as epoxide ring opening product, have been also detected (0.9–6.8%). In some extent, allylic oxidation has also occurred with the formation of 2-cyclohexene-1-ol and 2-cyclohexene-1-one. The alcohol derivative determined to be 1.1–2.8% and the yield of the corresponding ketone is 2.5–4.1%. Overall, cyclohexene is epoxidized by the present catalytic systems with 82–87% selectivity (see Fig. 6).

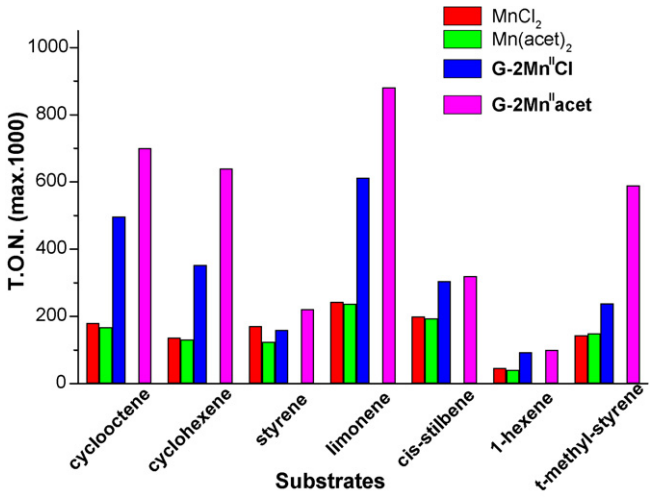


**Fig. 5.** Bar chart representation of alkene epoxidations catalysed by $MnCl_2$, $Mn(acet)_2$, $Mn(acet)_2/L_A$ **G-2Mn$^{II}$Cl** and **G-2Mn$^{II}$acet** in the presence of $H_2O_2$. Reaction performed in $CH_3COCH_3/CH_3OH$ (0.45:0.40 ml). See Table 1 for details.

Styrene oxidation produces mainly epoxide with yields from 16.0% to 47.6%, and 90–98% selectivity; small amounts of phenyl-acetaldehyde as side product have been detected. The catalysts showed analogous ability towards the oxidation of *trans*-methylstyrene resulted in 21.5–54.3% epoxide yield with >99% retention of its configuration. Small amounts of the corresponding methyl-ketone have been also observed (1.3–4.7%). The major products detected from oxidation of limonene, were two epoxides (*cis*- and *trans*-) derived from epoxidation of the electron-rich double bond in 1,2-position and two diastereoisomers derived from the more accessible but less electron-rich double bond in 8,9-position. Additionally, small amounts of products formed by allylic oxidation of the limonene ring have been observed. These were identified as the corresponding derivatives of cyclohexene-1-ol and cyclohexene-1-one. The total yield of epoxides (1,2- plus 8,9-) was varied from 39.9% to 87.5%. It is noted that an additional 0.9% of di-epoxide has been also formed. The corresponding cyclohexene-1-ol was detected from 0.7% to 2.0% and the corresponding cyclohexene-1-one from 0.8% to 1.1%. However, the epoxidation was clearly the main reaction path resulting mainly in 1,2-epoxides (see Table 1 and Fig. 6). In the oxidation of *cis*-stilbene, the major product was *cis*-epoxide with selectivity of 73–83% and yield ranging from 9.3% to 24.5%. Moreover, considerable amounts of *trans*-stilbene epoxide (1.3–4.2%) and 1,2-diphenyl ethanone (0.8–3.3) have been also detected.

When we inspect the influence of the R-substituents of the ligands **1** and **2** on the catalytic activity, we notice that the heterogeneous catalysts based on either of these ligands are almost equally efficient. This finding is in accordance with the catalytic data observed by the corresponding homogeneous systems; EPR data showed that the first coordination sphere of the Mn center was not affected by R-substituents. Therefore the side chain modifications play practically no-role in the catalytic activity [22].

When we evaluate the performance of the sol–gel material **S-1Mn$^{II}$Cl** and the corresponding grafting material **G-1Mn$^{II}$Cl** for alkene epoxidation based on the data of Table 1, no valid difference is observed.

Competitive reactions show alkene reactivity to increase with the electron density of the double bond when the

**Table 2**
Chemo- and region-selectivity in alkene epoxidation with $H_2O_2$ catalysed by **G-1Mn$^{II}$Cl**, **S-1Mn$^{II}$Cl**, **G-2Mn$^{II}$Cl**, **G-1Mn$^{II}$acet**, and **G-2Mn$^{II}$acet**[a].

| Alkene 1 | Alkene 2 | Epoxide 1/epoxide 2[b] | | | | |
|---|---|---|---|---|---|---|
| | | **G-1Mn$^{II}$Cl** | **S-1Mn$^{II}$Cl** | **G-2Mn$^{II}$Cl** | **G-1Mn$^{II}$acet** | **G-2Mn$^{II}$acet** |
| Styrene | *trans*-Methylstyrene | 0.79 | 0.59 | 0.65 | 0.83 | 0.85 |
| Styrene | *cis*-Stilbene | 1.40 | 1.67 | 1.16 | 1.45 | 1.47 |
| Cyclooctene | Styrene | 2.81 | 2.10 | 3.24 | 2.54 | 2.62 |
| Cyclooctene | Cyclohexene | 0.93 | 0.90 | 1.11 | 1.14 | 1.21 |
| Cyclohexene | Hex-1-ene | 18.77 | 15.10 | 15.20 | 13.83 | 12.96 |
| Cyclohexene | 1-Methylcyclohexene | 0.61 | 0.57 | 0.59 | 0.63 | 0.59 |
| *cis*-1,2-Limon. epox.[c] | *trans*-1,2-Limon. epox.[c] | 1.21 | 1.23 | 1.20 | 1.28 | 1.21 |
| 1,2-Limonene epoxide[d] | 8,9-Limonene epoxide[d] | 5.03 | 5.23 | 4.71 | 5.48 | 5.16 |

[a] Conditions-ratio of catalyst:$H_2O_2$:$CH_3COONH_4$:substrate = 1:2000:1000:1000; equivalent of catalyst = 1 μmol in 0.85 ml $CH_3COCH_3$:$CH_3OH$ (0.45:0.40). Reactions were usually complete within 18 h.
[b] Yields based on starting substrate.
[c] *cis*-1,2- *vs. trans*-1,2-Limonene epoxide.
[d] 1,2- *vs.* 8,9-Limonene epoxide.

more electron-rich olefin is oxidized preferentially, e.g. 1-methylcyclohexene > cyclohexene > hex-1-ene (Table 2). These data might be taken as evidence of the electrophilic nature of oxygen transfer from manganese-oxo intermediate to the olefinic double bond. However, additional effects of alkene shape are obvious. For example, styrene epoxidation favours *vs. cis*-stilbene-epoxidation and the electron-rich trisubstituted double bond of limonene in 1,2-position gives approximately five times more epoxides than the more accessible but less electron-rich double bond in 8,9-position. The reactivity of other substrate types was briefly investigated and the results are listed in Table 2.

### 3.3. Comparison of chloride- vs. acetate-heterogeneous catalysts

The data of Table 1 and Figs. 4 and 5 show an enhanced reactivity of the acetate-heterogeneous catalysts compared to the chloride-heterogeneous catalysts, e.g. by 15–20%. This shows that acetate has a beneficial influence on the heterogenized Mn-catalysts studied herein. Strikingly, the same Mn-catalysts in the homogeneous phase, showed no difference in their catalytic efficiency between chloride and acetate [22]. This shows that in the heterogenized catalysts, additional factors influence the catalytic activity, e.g. compared with the homogeneous Mn-systems. These factors can be (a) differences in the properties of the $Mn^{II}$-active center. However our EPR and FT-IR data show only minor differences in the properties of the Mn(II)-complexes. (b) Significantly higher surface areas measured for the acetate-heterogeneous catalysts (285 $m^2\,g^{-1}$ for the **G-1Mn$^{II}$acet**, and 277 $m^2\,g^{-1}$ for the **G-2Mn$^{II}$acet**) *vs.* the corresponding chloride-heterogeneous catalysts (203 $m^2\,g^{-1}$ for **G-1Mn$^{II}$Cl**, and 198 $m^2\,g^{-1}$ for **G-2Mn$^{II}$Cl**). Given that the catalysts present similar metal loading, we consider that the increased surface area is correlated with enhanced catalytic activity of the acetate-heterogeneous catalysts, in accordance with previous observations [3,26].

### 3.4. Comparison of hetero- vs. homogeneous catalysts

Comparing the present heterogeneous **1**- and **2**-based-manganese catalysts with the corresponding homogeneous **1**- and **2**-based-manganese catalysts [22], we observe that the heterogeneous systems lead to considerable epoxidation reactivity with hydrogen peroxide. Moreover, the heterogeneous-acetate-catalysts show enhanced catalytic activity compared with the corresponding homogeneous-acetate-catalysts. That is, heterogenization process preserves the catalytic properties of the active-manganese-centers for alkene epoxidation *vs.* the competitive $H_2O_2$ dismutation and, in some cases increases their reactivity.

Comparing the selectivity of the present heterogeneous catalysts with the corresponding homogeneous systems [22], we observe that the former prefer to epoxidize smaller substrate molecules rather than bulky substrates. For example, the ratio [styrene epoxide]/[*cis*-stilbene epoxide] varies from 1.16 to 1.67 for the heterogeneous catalysts (Table 2) *vs.* 0.73 to 0.99 for the corresponding homogeneous catalysts [22]. This tendency is enhanced by the sol–gel material **S-1Mn$^{II}$Cl** supporting the suggestion that the inorganic support prevents, in some extent, the substrate approach to the catalyst active center due to steric hindrance. However, in general, the heterogeneous catalysts *vs.* the homogeneous did not present dramatically different selectivity with regard to the molecular dimension of the substrates. This could be due to the elongate organic bridge which holds the active catalyst in some distance from the silica support. Moreover, the sol–gel material **S-1Mn$^{II}$Cl** and the grafting material **G-1Mn$^{II}$Cl** present similar behaviour indicating that the **S-1Mn$^{II}$Cl**-mediated catalysis is accomplished mainly by the exposed surface active centers.

### 3.5. Catalyst stability

Catalyst stability is of major concern in homogeneous and heterogeneous catalysis. In the present case, for the systems studied herein two phenomena were screened in detail:

(a) *Leaching on the Mn(II)-complexes from the $SiO_2$ support*: This was tested by the 'filtration method' out according to Valkenberg and Hölderich [3]. Accordingly, in typical catalytic experiments, after 2 h, the solid catalysts were filtered. Into the filtrate, the progress of the oxidation reaction was monitoring by GC. Our data showed that, no evolution of the studied reactions was observed in the filtrate. This ensures that no leaching of the active supported Mn(II)-component occurs. Thus, the obtained catalytic results derive exclusively from the heterogeneous catalysts.
(b) *Leaching of free Mn ions in solution*: The catalytic performance of the manganese salts $MnCl_2$ and $Mn(CH_3COO)_2$ as homogeneous catalysts was examined. For comparison the data are provided in Table 1, and Figs. 4 and 5. As shown in Figs. 4 and 5 the catalytic activity of the manganese salts in solution is much inferior than those of the heterogeneous catalysts.

Overall, the control experiments provide strong evidence that the observed catalytic results are derived by the heterogeneous catalysts and no leaching of the active component or demetallation occurs during the catalytic processes.

### 3.6. Catalyst recycling

It is known that reuse of heterogeneous catalysts as supported Schiff base complexes in epoxidation reactions is difficult and remains challenging [27,28]. In our systems, to control the behaviour of the heterogeneous catalysts after recycling, after a first use the **G-1Mn$^{II}$Cl** and **S-1Mn$^{II}$Cl** catalysts were filtered, washed, dried and reused under the same experimental conditions as in Table 1. The data show that both **G-1Mn$^{II}$Cl** and **S-1Mn$^{II}$Cl** suffered from significant loss of catalytic activity (>90%) after the first reuse. In epoxidation reactions, as noted, upon recycling both activity and selectivity deteriorate [27,28]. Often, upon epoxidation conditions fracture of the ligand occurs, which limits recyclability. Herein we provide further data which show that that ligand destruction is occurring under epoxidation conditions.

### 3.7. Characterisation of used catalysts

DRIFTS-IR and DR UV spectra of the used catalysts showed noticeable difference from the corresponding spectra of the unused **G-1Mn$^{II}$Cl** and **S-1Mn$^{II}$Cl** indicating significant structural modification of the organic ligands upon catalytic experiments. Moreover, changes in the TGA-profile of the used catalysts were observed. The EPR spectrum of the recycled **G-1Mn$^{II}$Cl** shows a severe linebroadening, see Fig. 1(iii). By measuring the EPR spectrum of centrifuged catalyst, we have verified that the broad EPR spectrum is due to $Mn^{II}$-ions on the $SiO_2$. This line broadening originates from non-specific spin–spin interactions between neighboring Mn spins and/or distributed *D*-values [22,29]. Thus the EPR data show that after the catalytic use of **G-1Mn$^{II}$Cl**, the manganese centers are randomly dispersed on the $SiO_2$ surface. Only a small percentage <10%, of mononuclear $Mn^{II}$ center are resolved showing that most (90%) of the **Mn$^{II}$1** complexes have been destroyed.

Overall, the data demonstrate that during the catalytic processes: (a) no leaching of the active-homogeneous catalysts occurs. (b) After extended catalytic activity, i.e. hundred TONs, oxidative destruction of the organic ligand occurs. (c) The Mn ions are randomly dispersed on the $SiO_2$ surface.

This shows that oxidative modification of the ligands is responsible for loss of catalytic activity of the recycled catalyst, after extended catalytic activity.

### 3.8. Mechanistic aspects

The EPR spectra in Fig. 1(i) and (ii) show that the coordination environment of the $Mn^{2+}$ centers is comparable in the homogeneous and heterogeneous catalysts. The low *D*-values show that the ligand field around the $Mn^{2+}$ is weak in both cases. Importantly this shows that the heterogenization, e.g. in **G-1Mn$^{II}$Cl**, does not alter the coordination environment of $Mn^{2+}$. A slightly stronger ligand field, i.e. evidenced by the increase in the *D*-value is the only effect of the heterogenization. Previously we have provided evidence that the low *D*-value for **Mn$^{II}$1** concurs with good catalytic activity [22]. In contrast a severe increase in *D*-value, indicative of a strong ligand-binding, has a severe inhibitory effect on the catalytic efficiency, as observed for oxalate additive [22].

This analysis shows that in the heterogeneous **G-1Mn$^{II}$Cl** catalyst the $Mn^{2+}$ center retains a flexible coordination environment as in the case of the homogenous **Mn$^{II}$1** catalyst. This explains the observed efficiency in catalytic activity as we show herein.

## 4. Conclusions

The symmetrical acetylacetone-based Schiff bases **1** and **2** were immobilized on a silica surface by two methods (a) grafting and (b) sol–gel procedure. The corresponding supported manganese complexes were prepared. The supported manganese complexes were evaluated as heterogeneous catalysts for alkene epoxidation with hydrogen peroxide and compared with the corresponding homogeneous systems published recently by our group [22].

The results obtained here demonstrate that the developed heterogeneous catalysts preserve the coordination and catalytic properties of the active-homogeneous manganese catalysts for alkene epoxidation *vs.* the competitive $H_2O_2$ dismutation. Moreover, the data show remarkable effectiveness and selectivity towards epoxide formation in the presence of ammonium acetate. This indicates that the active catalytic features of the homogeneous systems were successfully embedded onto the silica surface providing efficient heterogenized systems. EPR spectroscopy shows that a flexible, not-tight, coordination environment is characterising the Mn-complexes in both homo- and hetero-phase. However, the recycled catalysts suffer from significant loss of reactivity due to ligand modification during catalytic experiments. EPR shows that Mn ions are released and adsorbed randomly on the $SiO_2$ surface.

## Acknowledgement

The authors thank the postgraduate program "Bioinorganic Chemistry" at the Department of Chemistry, University of Ioannina.

## References

[1] G. Grigoropoulou, J.H. Clark, J.A. Elings, Green Chem. 5 (2003) 1–7.
[2] W.F. Holderich, F. Kollmer, Pure Appl. Chem. 72 (2000) 1273–1287.
[3] M.H. Valkenberg, W.F. Holderich, Catal. Rev. 44 (2002) 321–374.
[4] D.E. De Vos, B.F. Sels, P.A. Jacobs, Adv. Synth. Catal. 345 (2003) 457–473.
[5] D.E. De Vos, M. Dams, B.F. Sels, P.A. Jacobs, Chem. Rev. 102 (2002) 3615–3640.
[6] D. Brunel, N. Bellocq, P. Sutra, A. Cauvel, M. Lasperas, P. Moreau, F.D. Renzo, A. Galarneau, F. Fajula, Coord. Chem. Rev. 178–180 (1998) 1085–1108.
[7] J.S. Rafelt, J.H. Clark, Catal. Today 57 (2000) 33–44.
[8] J.H. Clark, D.J. Macquarrie, Chem. Commun. (1998) 853–860.
[9] D.E. De Vos, P.A. Jacobs, Catal. Today 57 (2000) 105–114.
[10] P.M. Price, J.H. Clark, D.J. Macquarrie, J. Chem. Soc., Dalton Trans. (2000) 101–110.
[11] P. Sutra, D. Brunel, Chem. Commun. (1996) 2485–2486.
[12] I.C. Chisem, J. Rafelt, M.T. Shieh, J. Chisem, J.H. Clark, R. Jachuck, D. Macquarrie, C. Ramshav, K. Scott, Chem. Commun. (1998) 1949–1950.
[13] X.-G. Zhou, X.-Q. Yu, J.-S. Huang, S.-G. Li, L.-S. Li, C.-M. Che, Chem. Commun. (1999) 1789–1790.
[14] P. Oliveira, A. Machado, A.M. Ramos, I.M. Fonseca, F.M. Braz Fernandes, A.M. Botelho do Rego, J. Vital, Catal. Commun. 8 (2007) 1366–1372.
[15] T.J. Terry, T.D.P. Sttack, J. Am. Chem. Soc. 130 (2008) 4945–4953.
[16] Y.V.S. Rao, D.E. De Vos, T. Bein, P.A. Jacobs, Chem. Commun. (1997) 355–356.
[17] M.A. Martinez-Lorente, P. Battioni, W. Kleemiss, J.F. Bartoli, D. Mansuy, J. Mol. Catal. A 113 (1996) 343–353.
[18] D. Zois, Ch. Vartzouma, Y. Deligiannakis, N. Hadjiliadis, L. Casella, E. Monzani, M. Louloudi, J. Mol. Catal. A 261 (2007) 306–317.
[19] Ch. Vartzouma, E. Evaggellou, Y. Sanakis, N. Hadjiliadis, M. Louloudi, J. Mol. Catal. A 263 (2007) 77–85.
[20] A. Serafimidou, A. Stamatis, M. Louloudi, Catal. Commun. 9 (2008) 35–39.
[21] M. Louloudi, Ch. Kolokytha, N. Hadjiliadis, J. Mol. Catal. A 180 (2002) 19.
[22] Ag. Stamatis, P. Doutsi, Ch. Vartzouma, K.C. Christoforidis, Y. Deligiannakis, M. Louloudi, J. Mol. Catal. A 297 (2009) 44–53.
[23] G.H. Reed, G.D. Markham, in: L.J. Berliner, J. Reuben (Eds.), Biological Magnetic Resonance, vol. 6, Plenum, New York, 1984, pp. 73–142.
[24] S. Misra, Physica B 203 (1994) 193–200.
[25] B.T. Allen, J. Chem. Phys. 43 (1965) 3820–3826.
[26] H. Chen, W.L. Dai, J.F. Deng, K. Fan, Catal. Lett. 81 (2002) 131–136.
[27] D.C. Sherrington, Catal. Today 57 (2000) 87–104.
[28] K.C. Gupta, A.K. Sutar, C.-C. Lin, Coord. Chem. Rev. 253 (2009) 1926–1946.
[29] A. Bencini, D. Gatteschi, Electron Paramagnetic Resonance of Exchange Coupled Systems, Springer-Verlag, Berlin, 1990.